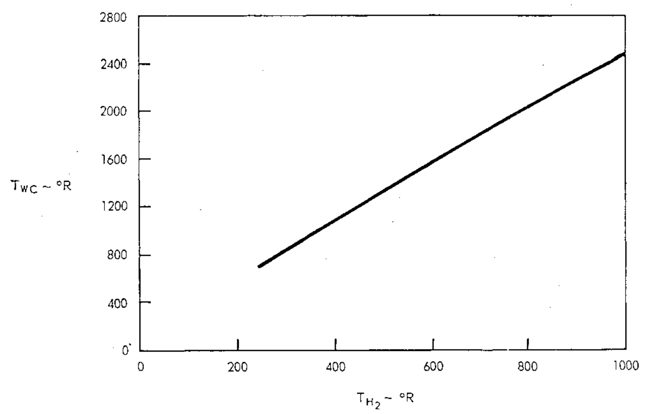

Fig. 1 Gaseous hydrogen coolant temperature to minimize flow for given T_{wc}.

$$\phi = (k_c)^{-0.6} (\mu_c/c_{pc})^{0.4} \tag{7}$$

For a given engine condition, with the dimensions of a coolant circuit fixed, θ = const. Equation (5) is differentiated to give

$$\frac{dw_c}{dT_c} = (\theta)^{1.25}(T_c)^{-0.6875} (T_{wc} - T_c)^{-1.25}(\phi)^{1.25} \times \left\{1.25\left[\frac{d\phi/dT_c}{\phi} + \frac{1}{T_{wc} - T_c}\right] - \frac{0.6875}{T_c}\right\} \tag{8}$$

$(dw_c/dT_c) = 0$ establishes the criterion for a minimum.

2. *Analysis with gaseous Hydrogen*

In order to solve Eq. (8), ϕ must be defined. Gaseous hydrogen at high pressure (500 psia) is assumed as the coolant. At high pressure c_{pc}, k_c, and μ_c are essentially independent of pressure. An approximate linear curve fit yields

$$\phi\ (T_{H_2}) \cong 0.521 - 7.73 \times 10^{-5}(T_{H_2}) \tag{9}$$

$$d\phi/dT_{H_2} \cong -7.73 \times 10^{-5} \tag{10}$$

Only one solution which is physically valid may be obtained from Eq. (8) when $(dw_c/dT_c) = 0$. The criterion for this solution is obtained from the term

$$1.25\left[\frac{d\phi/dT_{H_2}}{\phi} + \frac{1}{T_{wc} - T_{H_2}}\right] - \frac{0.6875}{T_{H_2}} = 0 \tag{11}$$

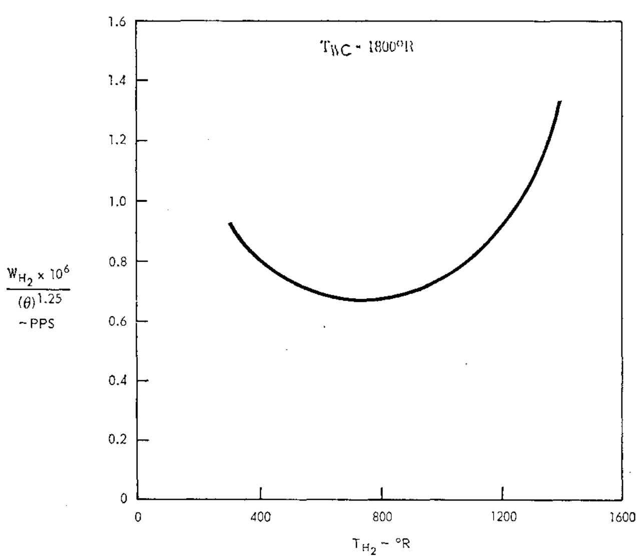

Fig. 2 Regenerative cooling flow variation with coolant temperature, T_{wc} = 1800°R.

Equation (11) is a quadratic in T_{H_2}, which yields the following solution

$$T_{H_2} = 1.90 \times 10^4 - 0.820(T_{wc}) - [3.61 \times 10^8 + 0.672 \times (T_{wc})^2 - 5.82 \times 10^4(T_{wc})]^{1/2} \tag{12}$$

Figure 1 is a plot of Eq. (12). Current hypersonic ramjet designs, utilizing regenerative cooling, employ T_{wc} values to 3000°R depending upon the application and the resulting material selection. For illustrative purposes a T_{wc} = 1800°R has been chosen. The variation of the coolant flow requirements with coolant (hydrogen) temperature at this condition is shown in Fig. 2.

Conclusions

A significant variation in hydrogen coolant flow requirements as a function of coolant temperature can occur in regeneratively cooled engines. Clever design of the coolant flow circuit can reduce the cooling flow rate more than 60% if the cryogenic hydrogen carried on the vehicle is properly elevated in temperature prior to cooling the throat of the nozzle.

References

[1] McCarthy, J. R. and Wolf, H., "The heat transfer characteristics of gaseous hydrogen and helium," Rocketdyne Research Rept. 60-12, p. 50 (December 1960).

[2] McAdams, W. H., *Heat Transmission* (McGraw-Hill Book Co., Inc., New York, 1954), 3rd ed., Chap. 8, pp. 184–188.

[3] Bartz, D. R., "An approximate solution of compressible turbulent boundary-layer development and convective heat transfer in convergent-divergent nozzles," Trans. Am. Soc. Mech. Engrs. **77**, 1235–1245 (1955).

Further Similarity Solutions of Two-Dimensional Wakes and Jets

Martin H. Steiger* and Karl Chen†
Polytechnic Institute of Brooklyn, Freeport, N. Y.

SOLUTIONS of the Falkner-Skan equation

$$f''' + ff'' + \beta[1 - f'^2] = 0 \tag{1a}$$

subject to the boundary conditions

$$f(0) = f''(0) = 0 \qquad f'(\infty) = 1.0 \tag{1b}$$

describe the two-dimensional, isoenergetic, symmetric viscous free mixing with streamwise pressure gradient under conditions of similarity, wherein

$$u = u_e(s)f'(\eta)$$

$$\eta = \frac{u_e}{(2s)^{1/2}}\int_0^y \rho dy \qquad s = \int_0^x \rho_e\mu_e u_e dx$$

$$\beta = \frac{2s}{u_e}\frac{du_e}{ds}\frac{H_e}{h_e} \qquad \rho\mu = \rho_e\mu_e$$

Primes denote total differentiation with respect to η and sub-

Received August 25, 1964. The study was supported by the Air Force Office of Scientific Research Grant No. AF-AFOSR-1-63. The authors acknowledge with thanks many useful discussions with Martin H. Bloom.

* Assistant Professor, Aerospace Engineering. Member AIAA.

† Research Fellow, Aerospace Engineering.

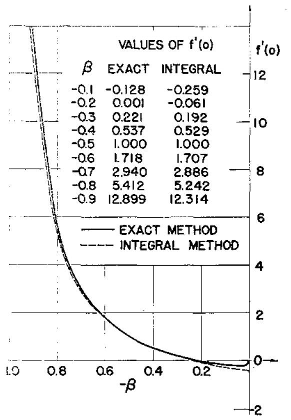

Fig. 1a Axis velocity $f'(0)$ vs pressure gradient parameter β; for $\beta \leq 0$.

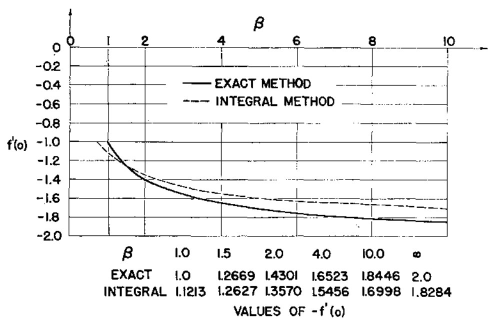

Fig. 1b Axis velocity $f'(0)$ vs pressure gradient parameter β; for $\beta \geq 0$.

script e denotes conditions at the edge of the viscous layer. Other symbols used here are defined in Sec. 8.2 of Ref. 4.

Stewartson[1, 2] and Kennedy[3] have investigated Eqs. (1) in the range $-0.5 \leq \beta \leq 0$. Lees and Reeves[5] and Kennedy[3] have noted that these solutions have some relevance to the laminar flow behind flat-based bodies.

Herein, solutions of Eqs. (1) in the ranges $-1.0 < \beta < -0.5$ and $1.0 < \beta$ are derived. Exact solutions (obtained by a forward numerical integration) and approximate integral method solutions are presented. The numerical integration utilized a fourth-order Runge-Kutta[6] scheme and a calculation procedure that is described in detail by Clutter and Smith.[7] Briefly, an initial value problem is formed by systematically specifying (for given β) $f'(0)$. The exact solution is extracted by requiring both the boundary condition $f'(\infty) = 1.0$ and the auxiliary condition $f''(\infty) = 0$ to be satisfied to three significant figures. The integral method helped facilitate solutions by providing a reasonable initial estimate for $f'(0)$. In addition, in order to insure uniqueness when $\beta < 0$, it was postulated that $f' \rightarrow 1$ exponentially as $\eta \rightarrow \infty$.

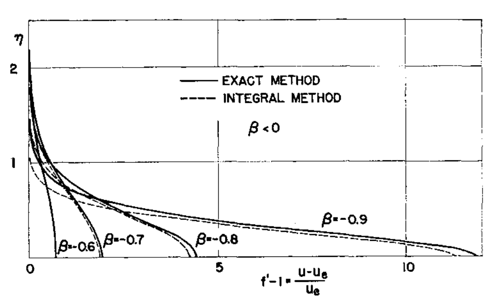

Fig. 2 Velocity profiles for $-1.0 < \beta < -0.5$.

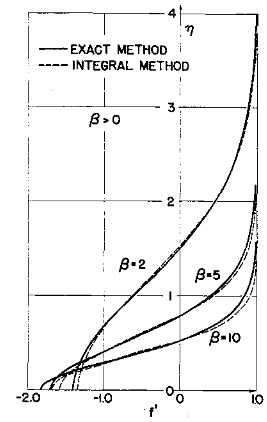

Fig. 3 Velocity profiles for $\beta > 1.0$.

The integral method solutions are facilitated with the analysis of Ref. 4. Direct integration of Eqs. (1a), with (1b) and $f''(\infty) = 0$ yields

$$\int_0^\infty f'(1 - f')d\eta + \beta \int_0^\infty (1 - f'^2)d\eta = 0 \qquad (2)$$

Approximate solutions are derived by assuming

$$f' = 1 + [f'(0) - 1]e^{-b\eta^2/2} \qquad (3)$$

where $f'(0)$ and b are constants. $f'(0)$ is determined by satisfying Eq. (2), and b is determined by evaluating Eq. (1a) at $\eta = 0$. There results

$$f'(0) = -\frac{(2^{1/2} - 1) + \beta(8^{1/2} - 1)}{1 + \beta} \qquad (4a)$$

$$b = -\beta[1 + f'(0)] \qquad (4b)$$

It is of interest to note that with (2) the following exact result can be derived:

$$\delta^*/\theta = -[(1 + \beta)/\beta]$$

for all β, where δ^* and θ are, respectively, the displacement and momentum thicknesses.

The pertinent results are presented in Figs. 1–3. The velocity at the axis $f'(0)$ is given as a function of the pressure gradient parameter β in Figs. 1a and 1b, and the f' profiles are shown in Figs. 2 and 3 for negative and positive values of β, respectively.

From Figs. 1a and 2 it is seen that, for $-1.0 < \beta < -0.5$, the velocity profiles are jet-like; that is, f' is greater than unity at $\eta = 0$ and decreases monotonically to unity as η increases from zero to infinity. It is noted that, as $\beta \rightarrow -1.0$, $f'(0) \rightarrow \infty$. There appear to be no reasons, either physical or mathematical, for ruling out these solutions.

When $1 < \beta < \infty$, Fig. 1b shows that $-1.0 < f'(0) < -2.0$. In this range of β, the velocity profiles (Fig. 3) are wake-like, wherein f' has a minimum at $\eta = 0$ and increases monotonically to unity as η increases from zero to infinity.

In general, the figures show good agreement between the approximate and exact solutions when $\beta < -0.1$ and when $\beta > 1$. In the range $-0.1 < \beta < 0$ estimates obtained with the simple form of integral method used here are not of acceptable accuracy; whereas in the range $0 < \beta < 1$, they yield inadmissable values of $b < 0$.

Conclusions concerning the existence of solutions when $0 < \beta < 1.0$ (and $\beta < -1.0$) have not been formulated. Clearly, a complete theoretical analysis on the existence of all possible solutions of Eqs. (1) would be of interest.

References

[1] Stewartson, K., "Further solutions of the Falkner-Skan equation," Proc. Cambridge Phil. Soc. **50,** 454–465 (1954).

[2] Stewartson, K., "Falkner-Skan equations for wakes," AIAA J. **7,** 1327–1328 (1964).

[3] Kennedy, E. D., "Wake-like solutions of the laminar boundary-layer equations," AIAA J. 2, 225–231 (1964).

[4] Hayes, W. and Probstein, R., *Hypersonic Flow Theory* (Academic Press Inc., New York, 1959), p. 321.

[5] Lees, L. and Reeves, B., "Supersonic separated and reattaching laminar flows: 1. General theory and application to adiabatic boundary layer-shock wave interaction," Firestone Flight Science Lab., Graduate Aeronautical Lab., California Institute of Technology TR 3, p. 36–37 (October 1963).

[6] Hildebrand, F. B., *Introduction to Numerical Analysis* (McGraw Hill Book Co., Inc., New York 1956), p. 237.

[7] Clutter, D. W. and Smith, A. M. D., "Solution of the general boundary-layer equations for compressible laminar flow, including transverse curvature," Douglas Aircraft Div. Rept. LB31088, p. 34–37 (February 1963).

Parameters Affecting the Normal Shock Location in Underexpanded Gas Jets

L. D'Attorre* and F. C. Harshbarger†
General Dynamics/Astronautics, San Diego, Calif.

Introduction

Recently the authors have completed an experimental and theoretical determination of the axial position of the normal shock formed by an underexpanded supersonic nozzle for a variety of different exit conditions and working fluids. Lewis and Carlson[1] have provided a semiempirical correlation that appears to be adequate for the one particular shape of nozzle studied and for a static ambient. The correlation may not be appropriate for other nozzle shapes or for a supersonic ambient.

Effect of Exit-Flow Angle

Lewis and Carlson[1] studied two 15° half-angle conical nozzles. One had an area ratio (exit to throat) of 1.385 and the other had an area ratio of 3.868. They utilized N_2, CO_2, and He as the working fluids. They found an excellent correlation between their results and the expression

$$x/d_e = k_1 M_e \gamma_e^{1/2} (p_e/p_a)^{k_2} \quad (1)$$

where x is the axial distance to the normal shock (measured from the nozzle exit plane), d_e is the nozzle exit diameter, M_e is the nozzle exit Mach number, γ_e is the ratio of specific heats at the nozzle exit, p_e is the static pressure at the nozzle exit, and p_a is the ambient static pressure. They found that $k_1 = 0.69$ and $k_2 = \frac{1}{2}$ provided a good fit to their data. Any effect of the exit flow angle is not provided explicitly in relation (1).

Recently[2–4] a number of additional theoretical and experimental determinations have been made for the axial distance to the normal shock utilizing both conically shaped nozzles and a nozzle with Foelsch coordinates.[5] The Foelsch shape is designed to provide axial flow (a zero flow angle) at the exit. The Foelsch nozzle was operated with two different gases ($\gamma_e = 1.225$ and $\gamma_e = 1.4$). The conical nozzles had both 6° and 15° half angles. The conical engines were operated with one gas, $\gamma_e = 1.225$. In addition, some shock positions were calculated (by the method of Bowyer, D'Attorre, and Yoshihara[6]) for conditions for which no experimental data were available.

It was discovered that, whereas the present data for a 15° half-angle conical nozzle can be correlated well with expression (1) with $k_1 = 0.69$ and $k_2 = \frac{1}{2}$, the Foelsch nozzle data falls outside the range of reasonable correlation with these values for the coefficients. The Foelsch data is correlated reasonably well by expression (1) if $k_1 = 0.813$ and $k_2 = \frac{5}{8}$. Only one data point was obtained for the 6° half-angle conical nozzle. It apparently falls outside the reasonable bounds of correlation for either the 15° conical or the Foelsch coordinate nozzles.

The result of this study suggests that the position of the normal shock is sensitive to the flow angle at the nozzle exit. This same conclusion was reached by Love.[7]

Received August 27, 1964. This investigation was sponsored by the Advanced Research Projects Agency, Department of Defense and the Office of Aerospace Research, U. S. Air Force.

* Staff Scientist, Space Science Laboratory.

† Senior Staff Scientist, Space Science Laboratory. Member AIAA.

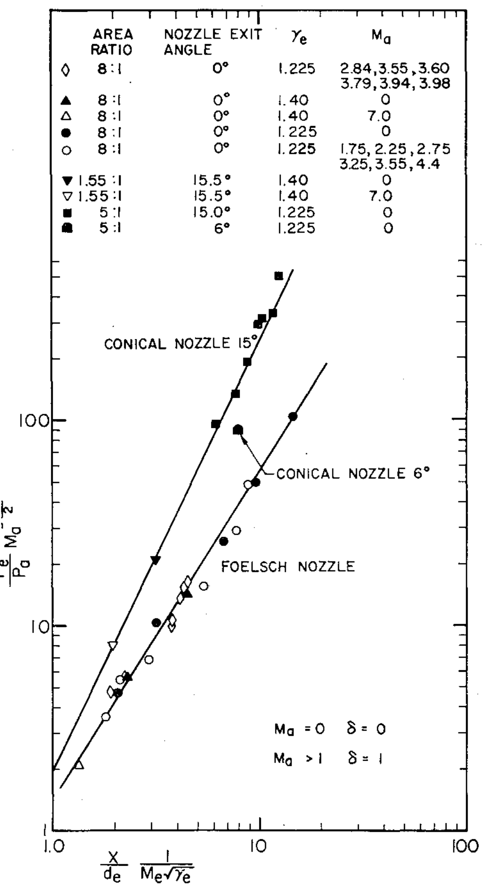

Fig. 1 Normalized experimental data for the axial position of the normal shock obtained from three different nozzle shapes.

Effect of a Supersonic Ambient

Experiments and calculations were conducted also with the 15° nozzle and the Foelsch nozzle with a supersonic ambient superimposed. As the ambient flow velocity was increased the distance to the normal shock decreased. A modification of relation (1) appears to be useful for correlating the data for conditions in which there is a supersonic ambient, i.e.,

$$x/d_e = k_1 M_e \gamma_e^{1/2} (p_e/p_a)^{k_2} M_a^{-1/2\delta k_2} \quad (2)$$

where $\delta = 0$ when $M_a = 0$, and $\delta = 1$ when $M_a > 1$.

In Fig. 1 is given a correlation between the present experimental and theoretical results and relation (2) for the three different nozzle shapes and for a variety of subsonic and supersonic ambient conditions. A straight line has been drawn through the data obtained from the Foelsch nozzle and from the 15° half-angle conical nozzle representing the two sets of coefficients. There is some scatter in the data in Fig. 1. This may be due in part to uncertainties in the actual operating conditions and in part to the method of deducing the actual position of the normal shock from the original photographs. Despite the scatter, it appears that a reason-